ARTICLE

Modulation of π character upon complexation captured by molecular rotation spectra

Received 00th January 20xx,
Accepted 00th January 20xx

DOI: 10.1039/x0xx00000x

Yang Zheng,[a,b] Qin Yang,[b] Sven Herbers,[c] Wanying Cheng,[a] Zhongming Jiang,[b] Hao Wang,[a] Xuefang Xu,[a] Julien Bloino*[b] and Qian Gou*[a,d]

Two configurations of the furan–CF_3Cl complex have been observed by high-resolution rotational spectroscopy. One is characterized by a dominant Cl lone pairs···π*aromatic interaction and the other is stabilized by a C-Cl···π-C=C- halogen bond. This is the first rotational spectroscopic evidence, to the best of our knowledge, that shows how a complexation with a partner like CF_3Cl (the weak lone pair belt of Cl, to be more specific) can both facilitate the aromatic π* and diene π characters of a heteroaromatic molecule. The results emphasize the partner molecules' role in modulating the π electron structure and will not only deepen our understanding on non-covalent interactions but also lead to better designs of heteroaromatic-based drugs and materials.

Introduction

Noncovalent interactions (NCIs) involving aromatic π systems have drawn considerable attention because of their widespread presence and paramount roles in determining the selectivity of asymmetric transformations,[1] the formations and structures of pre-reactive intermediates,[2] the folding of proteins,[3] the mechanism of catalysis,[4] the discrimination of chiral molecules,[5] and the function of materials,[6] to name a few. Complexes of benzene and its derivatives have carved out a niche in prototypical studies of aromatic π interactions,[7-9] which lay the foundation for rationally building into a wide variety of architectures and assemblies for macroscopic systems.[5,10] For this purpose, Fourier transform microwave (FTMW) combined with a supersonic molecular jet expansion gives unique insights into different NCIs from their structural and energetic signatures.[11,12] The unique spectral patterns stem from its high sensitivity to changes in the moments of inertia and thus to the overall mass distribution of weakly-bonded molecular complexes. Since the interaction sites and the relative arrangement of the moieties are determined in isolation, free from solvent effects or lattice strain, the method allows identifying accurately the intermolecular forces at play.

It has been emphasized, indeed, based on rotational spectroscopic studies, that NCIs strengths and even topologies can be finely tuned through substituent effects by varying the electron distribution and symmetry of the aromatic rings. A consensus has been reached that the electron-withdrawing substituents are pulling electron density from the aromatic ring through π resonance effects and make it a weaker electron donor in formation of NCIs, and vice versa. Pushed to the limits, the benzene rings can be tuned by the electron withdrawing perhalogenation, creating an electron-deficient aromatic surface("π-hole") steering the π* orbitals to link with an electronegative site, known as lone pair (LP)···π* or Bürgi–Dunitz n–π* interaction.[13] Such effect has also been found in perhalogenated pyridinic[14,15] and vinyl π systems.[16] While most attention has been drawn to the substitution effect, a recent rotational study has revealed that the benzenic π feature of benzaldehyde is switched to π* by complexation with high electronegativity like CF_4, forming the LP···π* interaction.[17] The results highlighted the modulation effect of the complexation on the π electron structures in the formation of NCIs.

Furan is one of the simplest heterocyclic aromatic molecules following Hückel's (4*n*+2) π-electron rule, where the oxygen atom contributes one lone pair of π-electrons to the π system creating a 6π electron aromatic molecule. Its high reactivity makes it a privileged scaffold in many bioactive natural products exhibiting pharmaceutical activities.[18] With the O atom and the heteroaromatic ring acting as the electron donors, complexes of furan might form σ-[19,20] or π-[21-26] types configurations. For example, HF[20] and HCl[19] link with the O atom of furan through an in-plane F/Cl-H···O HB to form σ-type complexes with furan behaving like an ether, while with HBr,[21] the π type configuration is favored, characterized by a Br-H···$\pi_{aromatic}$ HB, where furan acts like benzene.[27] It seems that the lower electronegativity of the Br atom with respect to F or Cl makes HBr a weaker proton donor which is favored by the furan aromatic π system rather than the O atom. Such preference of π electrons has also been found in the complexes of furan with other weak proton donors like ethylene[22] and methanol,[23] and

[a] *Department of Chemistry, School of Chemistry and Chemical Engineering, Chongqing University, No.55 Daxuecheng South Rd., Shapingba, Chongqing, 401331, China.*
[b] *Scuola Normale Superiore di Pisa, Piazza dei Cavalieri 7, 56125 Pisa, Italy.*
[c] *Institute for Molecules and Materials, Radboud University, Heijendaalseweg 135, NL-6525 AJ Nijmegen, Netherlands.*
[d] *Chongqing Key Laboratory of Theoretical and Computational Chemistry, Chongqing University, 401331 Chongqing, China.*
† Electronic Supplementary Information (ESI) available. See DOI: 10.1039/x0xx00000x

with weak electron acceptors, like CO,[24] and SO_2.[25] Surprisingly, although furan is often considered as an aromatic molecule, it acts more like a diene when linking with ClF, where only one of the -C=C- bonds participates in forming the F-Cl···π halogen bond (HaB).[26] Beside the linear ClF, CF_3Cl has been frequently taken as the prototypical halogen donor in studies of HaBs,[28] due to the "σ hole" induced by the electron withdrawing effect of the three F atoms being collinear with the C–Cl bond. A recent rotational study has revealed that the lone pairs of Cl around its "equatorial belt" can also act as a weak electron donor and link with the π-hole of CO_2,[29] reminding us that the negative lateral side of Cl should be more carefully considered when it comes to elucidating NCIs.

In order to study how the partner molecule like CF_3Cl interacts with furan, resulting what kind of NCIs and configurations between them, we thus conducted the rotational spectroscopic study on the complex. This study shows, to the best of our knowledge, that the electronegative molecule CF_3Cl can modulate both aromatic π* and diene π characters of the furan ring when participating in NCIs. This study gives us a deeper impression of the important role of the partner molecule. The details are reported below.

Experimental and computational details

Experimental

Commercial samples of furan and CF_3Cl were used without further purification. Molecular clusters of furan–CF_3Cl were generated in a supersonic expansion, under optimized conditions. Details of the Fourier transform microwave (FTMW)[30] spectrometer (COBRA-type),[31] which covers the 2-20 GHz range, have been described previously.[32] A 1:1 gas mixture of furan and CF_3Cl at a concentration of ~1.5% in helium (or neon) and a stagnation pressure of ~0.15 MPa was expanded through a solenoid valve (General Valve, Series 9, nozzle diameter 0.5 mm) into the Fabry-Pérot cavity (the pressure of the cavity is ~10^{-5} Pa). The spectral line positions were determined after Fourier transformation of the time-domain signal with 8k data points, recorded with 100 ns sample intervals. Each rotational transition appears as a doublet because of the Doppler Effect. The line position is calculated as the arithmetic mean of the frequencies of the Doppler components.

Computational

Prior to recording the rotational experiments, a conformational search was carried out using the CREST tools[33] to sample the conformational space of the target complex. The resulting candidates were then optimized at the *rev*DSD-PBEP86-D3(BJ)[34]/jun-cc-pVTZ (abbreviated as rDSDj) level, using a locally modified version of Gaussian 16.[35] Harmonic frequency calculations at the same level were carried out to confirm these isomers to be real minima with the absence of imaginary frequencies, providing the zero-point energy (ZPE).

Johnson's NCI analysis[36] was first applied by using the Multiwfn program[37] to have a graphical representation of the intermolecular interactions occurring in the furan–CF_3Cl complex. Natural Bond Orbital (NBO) analysis was performed using the NBO7 program[38] interfaced to Gaussian16, at the B3LYP-D3(BJ)[39]/aug-cc-pVTZ level. Symmetry adapted perturbation theory (SAPT)[40] approach, at the SAPT2+(3)/aug-cc-pVTZ level, as implemented in the PSI4 program package,[41] was done to have the interaction energy decomposition analysis.

Results and discussion

Theoretical calculations

Nine isomers were obtained at the rDSDj level, as shown in Fig. 1, which also displays the relative zero-point corrected energies of the different isomers. CF_3Cl prefers to be loosely anchored above the furan ring. These nine isomers can be cataloged into three classes according to the interaction sites of CF_3Cl involved in the NCIs with furan: 1) the Cl "equatorial belt" induced by its lone pairs (isomers I, II, V and VI); 2) the Cl σ-hole (isomers III and IV) acting as the halogen donor; 3) the C σ-hole (isomers VII, VIII and IX) serving as the electron acceptor. The equilibrium parameters of the nine isomers at the rDSDj level are reported in Table S1 of the Electronic Supplementary Information (ESI).

It is noteworthy that the rotational constants of some isomers are quite close to each other, for example those of isomers III and IV. In addition, the energy window of the nine isomers is within ~ 3 kJ mol^{-1}, which raises difficulties for the conformational assignment. In order to have a more accurate theoretical result to help with the identification, a hybrid approach (labelled as rDSDj/B3j) was employed and applied to isomers I, III and IV. This scheme combines the harmonic force field at the rDSDj level with anharmonic constants computed at the B3LYP-D3(BJ)[33]/jun-cc-pVTZ level. Previous study has highlighted the quality of such a method for the study of NCIs[42] while keeping the overall computational cost of such a procedure tractable even with limited hardware resources.

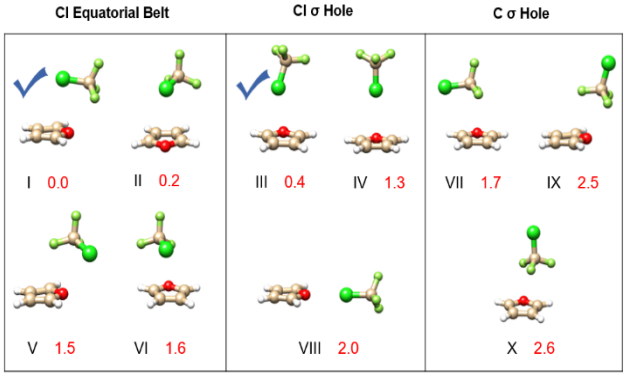

Fig. 1 Configurations of nine plausible isomers of furan–CF_3Cl predicted at the rDSDj level. The relative zero-point corrected energies at rDSDj level are given with the unit of kJ mol^{-1}. The isomers with the checkmarks have been experimentally observed in pulsed jets.

Rotational spectra

Two sets of spectra were observed and assigned in pulsed jet with helium as the carrier gas. The characteristic ^{35}Cl nuclear hyperfine structure patterns, as shown in Fig. 2 with the $8_{17} \leftarrow 7_{16}$ rotational transitions for both observed isomers, helped with initial assignments. It is straightforward to assign the first set of rotational spectrum to isomer I by comparing the values of the experimental rotational constants (A_0, B_0, and C_0 in Table 1) with the equilibrium ones (A_e, B_e, and C_e in Table S1 of the ESI) at the rDSDj level. We could then assign the spectrum of the ^{37}Cl isotopologue of isomer I in natural abundance (~ 24.23%). For the remaining spectral lines, both harmonic and anharmonic calculations give close rotational constants for isomers III and IV. Nevertheless, two aspects make isomer III a more likely candidate. First, isomer III has a much lower energy than isomer IV. Second, the discrepancies between the theoretical rotational constants with anharmonic simulations and experimental ones are in line with those found for isomer I, which hints at a consistent discrepancy of rDSDj in the description of the furan-CF_3Cl complex.[43] The undetermined value of the rotational constant A_0 can be attributed to the fact that only *a*-type transitions have been measured which are not sensitive to A_0. Therefore, its value was fixed at the calculated one based on the deviation pattern (0.7%) of isomer I. The equilibrium structures of isomers I and III are reported in Table S2 of the ESI.

The relative conformational populations prior to the jet expansion can be roughly estimated from the relative intensity measurements of the rotational transitions with helium as the carrier gas (see Table S3) allowed estimating the relative populations of the observed two isomers I and III in the pulsed jet, to be ~1.85/1.

A conformational relaxation from isomer III to isomer I occurred when the carrier gas was replaced by neon, which further confirmed isomer I to be the global minimum. We could thus measure three additional ^{13}C mono-substituted isotopologues (two *ortho*- and two *meta*-C in furan are identical) of isomer I with their natural abundance (~ 1.1%) in neon. Since a smaller number of lines that can be measured for the three ^{13}C isotopologues, the values of the quadrupole coupling and centrifugal distortion constants were set to those of the parent species. The full spectroscopic parameters of isomers I (including three ^{13}C and one ^{37}Cl isotopologues) and III are summarized in Table S4.

The spectroscopic fitting procedures were finished with the SPFIT program,[44] using Watson's semi-rigid rotor Hamiltonian in the *S*–reduction and I^r representation.[45] The measured rotational transition frequencies for both observed isomers are reported in Tables S5–S9.

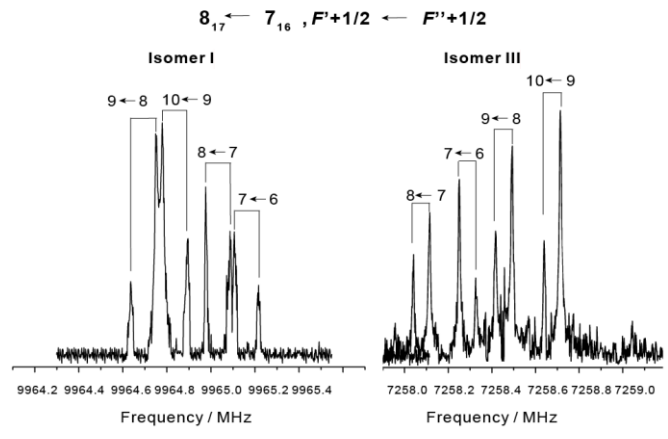

Fig. 2 Selected $8_{17} \leftarrow 7_{16}$ rotational transition of the two observed isomers I and III of furan–CF_3Cl, showing the ^{35}Cl (I = 3/2) nuclear hyperfine structures. Each line displays the Doppler doubling.

Table 1 Experimental and theoretical rotational and nuclear quadrupole coupling constants of the normal species of the observed isomers of furan–CF_3Cl[a]

		Isomer I
	EXP. 1	**rDSDj/B3j[b]**
A_0/MHz	2248.91(1)[c]	2232 (0.7%)
B_0/MHz	628.91(1)	642 (-2.2%)
C_0/MHz	606.00(1)	618 (-2.0%)
χ_{aa}/MHz	9.66(1)	8.41
$(\chi_{bb}-\chi_{cc})$/MHz	-86.06(1)	-81.53
$\lvert\chi_{ab}\rvert$/MHz	50.89(3)	48.62
σ/kHz[e]	3.5	
$N_{transtions}/N_{lines}$[f]	88/350	
		Isomer III **Isomer IV**
	EXP. 2	**rDSDj/B3j[b]** **rDSDj/B3j[b]**
A_0/MHz	[2447][d]	2430 2452
B_0/MHz	454.14(1)	463 (-1.9%) 449 (1.1%)
C_0/MHz	452.29(1)	461 (-2.0%) 447 (1.1%)
χ_{aa}/MHz	-71.5(5)	-64.62 -63.44
$(\chi_{bb}-\chi_{cc})$/MHz	--	-8.92 -10.34
$\lvert\chi_{ab}\rvert$/MHz	--	30.23 32.52
σ/kHz[e]	6.0	
$N_{transtions}/N_{lines}$[f]	25/100	

[a] Full table of spectroscopic parameters including centrifugal distortion constants are given in Table S4 of the ESI. [b] Vibrationally averaged rotational constants obtained by correcting the equilibrium rDSDj rotational constants for vibrational corrections at the B3j level. [c] Uncertainties (in parentheses) are 1σ uncertainties expressed in units of the last digit. [d] The value of rotational constant *A* for isomer III was fixed at the calculated value which is based on the deviation pattern (0.7%) of isomer I. [e] Root mean square deviation (in kHz) of the fit. [f] Number of transitions/lines in the fit.

Noncovalent interaction

The first observation from Fig. 3, based on the NCI analyses is that the two fragments bind together in markedly different ways between the two isomers. The NBO results of the two observed isomers give us a guide for the interaction types, as shown in Table S10 in ESI. The dominant interaction in isomer I is collectively characterized to be of Cl LP···$\pi^*_{aromatic}$ interaction, because, as marked in bold, the LPs of Cl link with the antibonding orbitals of furan's two double bonds and two O-C bonds. A secondary interaction between the C σ-hole of CF_3Cl and the LP of the oxygen of furan also contributes to the stability of isomer I. In isomer III, instead, the dominant interaction is Cl σ hole···$\pi_{-c=c-}$ HaB, the same as what has been found in the complex of furan–ClF.[26]

SAPT method, which can provide information on the nature of the binding contributions including electrostatics (E_{elec}), induction (E_{ind}), dispersion (E_{disp}), and exchange-repulsion (E_{ex})

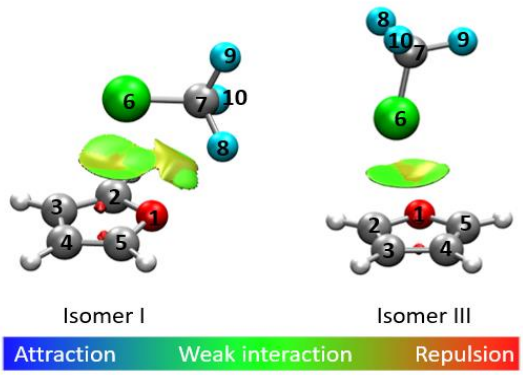

Fig. 2 NCI analysis of the isomers I and III of furan–CF_3Cl. The atom numbering of heavy atoms is also given. The isosurfaces correspond to the 0.5 a.u. isovalue and are colored according to the BGR scheme over the range −0.04 a.u. < sign(λ_2)ρ < 0.02 a.u.

components, was applied to both observed isomers of furan–CF_3Cl, as summarized in Table 2. The following conclusions can be drawn: Dispersion interactions play a crucial role in both isomers, accounting for 67.2% for isomer I and 55.7% for isomer III, respectively. The electrostatics contribute by 28.6% and 33.7% for I and III, respectively. Induction in isomer I has a negligible role, being 4.2%, but represents 10.6% in isomer III. The total binding energies of the two isomers are comparable, with a difference of ~0.7 kJ mol^{-1}, in agreement with the zero-point corrected relative energies (Fig. 1). In addition, the interaction energy of isomer III is stronger than that of isomer IV, further confirming the experimental identification of isomer III. The primary contribution in isomer I of furan–CF_3Cl is the same as that of benzaldehyde–CF_4 (BA–CF_4),[17] where the dispersion accounts for over 60%.

Table 2 Results of the SAPT2+(3)/aug-cc-pVDZ-RI calculations for isomers I, III and IV of furan–CF_3Cl, compared with those of BA–CF_4.[17] All values are given in kJ·mol^{-1}

Isomers	E_{elec}	E_{ex}	E_{ind}	E_{disp}	E_{tot}
I	−7.4 (28.6%)[a]	14.2	−1.1 (4.2%)	**−17.4 (67.2%)**	−11.7
III	−8.9 (33.7%)	15.4	−2.8 (10.6%)	−14.7 (55.7%)	-11.0
IV	−6.2 (29.5%)	10.7	−1.7 (8.1%)	−13.1 (62.4%)	-10.3
BA-CF_4	−4.7 (24.0%)	12.1	−0.6 (3.0%)	**−14.3 (73.0%)**	-7.5

[a] The values in parentheses represent the contributions to the total interaction energies

Conclusions

This rotational spectroscopic study, benefit from its direct relation between spectral patterns and molecular geometries, provides irrefutable experimental evidence on the modulation of furan π characters by complexation with CF_3Cl. Although furan is generally regarded as a heteroaromatic molecule, its π character can be more sophisticated than one might expect, when linking with specific partner molecules. Indeed, with Cl LPs of CF_3Cl, furan manifests itself as a heteroaromatic π* orbital in forming a dominant LP···$\pi^*_{aromatic}$ interaction (isomer I). However, with the Cl "σ-hole" of CF_3Cl, furan lends one of its C=C and participates in the formation of the Cl···$\pi_{C=C}$ halogen bond, acting like a diene (isomer III). It is worth mentioning that, due to the electron withdrawal F atoms of CF_3Cl, the electron density of the Cl "equatorial belt" is much lower than that of the F atoms. A weaker electron donor is preferred and able to switch π to π*, which might also give a hint on understanding of the nature of ambiguous π-π stacking interactions.[7,9] For example, in benzene dimer, the aromatic π electrons of one moiety might serve as the modulator to switch π to π* of the other so that a π···π* interaction contributes to its stability. The results gathered on the modulation of the π character of furan by complexation with CF_3Cl would not only deepen our understanding on NCI topologies but also inspire new thoughts in designing heteroaromatic-based drugs and materials.

Conflicts of interest

There are no conflicts to declare.

Acknowledgements

We are grateful for the financial supports from the National Natural Science Foundation of China (Grant Nos. U1931104 and 22073013), Fundamental Research Funds for the Central Universities (Grant No. 2020CDJXZ002), Chongqing Talents: Exceptional Young Talents Project (Grant No. cstc2021ycjh-bgzxm0027). Yang also thanks the China Scholarships Council (CSC) for financial support. We thank Marco Fusè for the help in writing *ad hoc* tools to process the data generated by CREST and Lorenzo Spada for the help on the spectral assignments. The SMART@SNS Laboratory (http://smart.sns.it) is acknowledged for providing high-performance computing facilities.

Notes and references

1 A. Erkkila, I. Majander and P. M. Pihko, *Chem. Rev.*, 2007, **107**, 5416-5470.
2 W. B. Bakr and C. D. Sherrill, *Phys. Chem. Chem. Phys.*, 2016, **18**, 10297-10308.
3 X. Lucas, A. Bauzá, A. Frontera and D. Quinonero, *Chem. Sci.*, 2016, **7**, 1038-1050.
4 N. Luo, Y. F. Ao, D. X. Wang and Q. Q. Wang, *Angew. Chem., Int. Ed.*, 2021, **60**, 20650-20655.
5 A. J. Neel, M. J. Hilton, M. S. Sigman and F. D. Toste, *Nature*, 2017, **543**, 637-646.
6 D. Umadevi, S. Panigrahi and G. N. Sastry, *Acc. Chem. Res.*, 2014, **47**, 2574−2581.
7 M. Schnell, U. Erlekam, P. Bunker, G. von Helden, J. U. Grabow, G. Meijer and A. Van Der Avoird, *Angew. Chem., Int. Ed.*, 2013, **52**, 5180-5183.
8 M. Schnell, U. Erlekam, P. R. Bunker, G. von Helden, J. U. Grabow, G. Meijer and A. van der Avoird, *Phys. Chem. Chem. Phys.*, 2013, **15**, 10207-10223.
9 R. T. Saragi, M. Juanes, C. Pérez, P. Pinacho, D. S. Tikhonov, W. Caminati, M. Schnell and A. Lesarri, *J. Phys. Chem. Lett.*, 2021, **12**, 1367-1373.
10 J. Šponer, J. E. Šponer, A. Mládek, P. Jurečka, P. Banáš and M. Otyepka, *Biopolymers*, 2013, **99**, 978-988.

11 M. Quack and F. Merkt Eds., *Handbook of High-Resolution Spectroscopy*, Wiley, 2011.
12 F. Xie, N. A. Seifert, W. Jäger and Y. Xu, *Angew. Chem., Int. Ed.*, 2020, **59**, 15703-15710.
13 L. Evangelisti, K. Brendel, H. Mäder, W. Caminati and S. Melandri, *Angew. Chem. Int. Ed.*, 2017, **56**, 13699-13703.
14 C. Calabrese, Q. Gou, A. Maris, W. Caminati and S. Melandri, *J. Phys. Chem. Lett.*, 2016, **7**, 1513-1517.
15 W. Li, I. Usabiaga, C. Calabrese, L. Evangelisti, A. Maris, L. B. Favero and S. Melandri, *Phys. Chem. Chem. Phys.*, 2021, **23**, 9121-9129.
16 Q. Gou, G. Feng, L. Evangelisti and W. Caminati, *Angew. Chem., Int. Ed.*, 2013, **52**, 11888-11891.
17 H. Wang, J. Chen, C. Duan, X. Xu, Y. Zheng, J.-U. Grabow, Q. Gou and W. Caminati, *J. Phys. Chem. Lett.*, 2021, **12**, 5150-5155.
18 T. Montagnon, M. Tofi and G. Vassilikogiannakis, *Acc. Chem. Res.*, 2008, **41**, 1001-1011.
19 J. A. Shea and S. G. Kukolich, *J. Chem. Phys.*, 1983, **78**, 3545-3551.
20 A. Lesarri, J. C. López and J. L. Alonso, *J. Chem. Soc., Faraday Trans.* 1998, **94**, 729-733.
21 G. C. Cole, A. C. Legon and P. Ottaviani, *J. Chem. Phys.*, 2002, **117**, 2790-2799.
22 S. Firth and R. L. Kuczkowski, *J. Chem. Soc., Faraday Trans.*, 1995, **91**, 975-981.
23 H. C. Gottschalk, A. Poblotzki, M. Fatima, D. A. Obenchain, C. Perez, J. Antony, A. A. Auer, L. Baptista, D. M. Benoit, G. Bistoni, F. Bohle, R. Dahmani, D. Firaha, S. Grimme, A. Hansen, M. E. Harding, M. Hochlaf, C. Holzer, G. Jansen, W. Klopper, W. A. Kopp, M. Krasowska, L. C. Kroger, K. Leonhard, M. Mogren Al-Mogren, H. Mouhib, F. Neese, M. N. Pereira, M. Prakash, I. S. Ulusoy, R. A. Mata, M. A. Suhm and M. Schnell, *J. Chem. Phys.*, 2020, **152**, 164303.
24 T. Brupbacher, J. Makarewicz and A. Bauder, *J. Chem. Phys.*, 1998, **108**, 3932-3939.
25 J. J. Oh, L. W. Xu, A. Taleb-Bendiab, K. W. Hillig II and R. L. Kuczkowski, *J. Mol. Spectrosc.*, 1992, **153**, 497-510.
26 S. A. Cooke, G. K. Corlett, J. H. Holloway and A. C. Legon, *J. Chem. Soc., Faraday Trans.*, 1998, **94**, 2675-2680.
27 S. A. Cooke, G. K. Corlett, C. M. Evans and A. C. Legon, *Chem. Phys. Lett.*, 1997, **272**, 61-68.
28 P. Politzer, P. Lane, M. C. Concha, Y. Ma and J. S. Murray, *J. Mol. Model.*, 2007, **13**, 305-311.
29 Y. Zheng, S. Herbers, Q. Gou, W. Caminati and J.-U. Grabow, *J. Phys. Chem. Lett.*, 2021, **12**, 3907-3913.
30 J. U. Grabow, W. Stahl and H. Dreizler, *Rev. Sci. Instrum.*, 1996, **67**, 4072-4084.
31 T. J. Balle and W. H. Flygare, *Rev. Sci. Instrum.*, 1981, **52**, 33-45.
32 J.-U. Grabow, Q. Gou and G. Feng, 72nd International Symposium on Molecular Spectroscopy, 2017, TH03.
33 P. Pracht, F. Bohle, and S. Grimme, *Phys. Chem. Chem. Phys.*, 2020, **22**, 7169–7192.
34 G. Santra, N. Sylvetsky and J. M. Martin, *J. Phys. Chem. A*, 2019, **123**, 5129-5143.
35 Gaussian Development Version, Revision, J.14, M. J. Frisch, G. W. Trucks, H. B. Schlegel, G. E. Scuseria, M. A. Robb, J. R. Cheeseman, G. Scalmani, V. Barone, G. A. Petersson, H. Nakatsuji et al., Gaussian, Inc., Wallingford CT, 2020.
36 E. R. Johnson, S. Keinan, P. Mori-Sánchez, J. Contreras-García, A. J. Cohen and W. Yang, *J. Am. Chem. Soc.*, 2010, **132**, 6498-6506.
37 T. Lu and F. Chen, *J. Comput. Chem.*, 2012, **33**, 580-592.
38 E. D. Glendening, C. R. Landis and F. Weinhold, *WIREs Comput. Mol. Sci*. 2012, **2**, 1–42.
39 S. Grimme, S. Ehrlich and L. Goerigk, *J. Comput. Chem.*, 2011, **32**, 1456-1465.
40 B. Jeziorski, R. Moszynski and K. Szalewicz, *Chem. Rev.*, 1994, **94**, 1887-1930.
41 R. M. Parrish, L. A. Burns, D. G. Smith, A. C. Simmonett, A. E. DePrince III, E. G. Hohenstein, U. Bozkaya, A. Y. Sokolov, R. Di Remigio and R. M. Richard, *J. Chem. Theory Comput.*, 2017, **13**, 3185-3197.
42 F. Xie, M. Fuse, A. S. Hazrah, W. Jager, V. Barone and Y. Xu, *Angew. Chem., Int. Ed.*, 2020, **59**, 22427-22430.
43 J. Bloino, M. Biczysko and V. Barone *J. Chem. Theory Comput.*, 2012, **8**, 1015-1036.
44 H. M. Pickett, *J. Mol. Spectrosc.*, 1991, **148**, 371–377.
45 J. K. G. Watson, In Vibrational Spectra and Structure; Durig, J. R., Ed.; Elsevier: New York/Amsterdam, 1977; Vol. 6, pp 1–89